# Models of the Cytochromes *b*. 4. Effect of Axial Ligand Plane Orientation on the Proton NMR Spectra of Symmetrically Substituted Low-Spin Iron(III) Porphyrins

**F. Ann Walker,*†[1] Joanne Buehler,† Joyce T. West,† and John L. Hinds‡**

*Contribution from the Department of Chemistry, San Francisco State University, San Francisco, California 94132, and Department of Chemistry, University of California, Berkeley, Berkeley, California 94720.* *Received March 4, 1982*

**Abstract:** Mixtures of the $\alpha\beta\alpha\beta$ and $\alpha\alpha\beta\beta$ atropisomers of tetrakis(*o*-pivalamidophenyl)porphyrin, $(o\text{-piv})_4TPPH_2$, were separated from the other atropisomers and the ratio determined by NMR techniques. Insertion of iron required extended reflux time, and significant (ca. 45–55%) atropisomerization to the $\alpha\alpha\alpha\beta$ isomer occurred based upon NMR spectra of the high-spin $((o\text{-piv})_4TPP)FeCl$ products and their low-spin bis(*N*-methylimidazole) adducts. Addition of small amounts of *N*-methylimidazole shifted the characteristic NMR peaks of the high-spin form in such a way as to indicate that the mono(*N*-methylimidazole) complex is predominantly in the five-coordinate, chloride-dissociated form. In the presence of a large excess of *N*-methylimidazole (0.6 M), four low-spin pyrrole proton resonances are observed. These resonances have been assigned to the $\alpha\beta\alpha\beta$ (−18.6 ppm), $\alpha\alpha\beta\beta$ (−17.1 and −20.0 ppm), and $\alpha\alpha\alpha\beta$ (−19.5 ppm) atropisomers. (It should be noted that the two peaks due to the $\alpha\alpha\beta\beta$ atropisomer are symmetrically displaced upfield and downfield from that of the $\alpha\beta\alpha\beta$ atropisomer.) Since the unpaired electron of low-spin Fe(III) porphyrins is known to be delocalized into the $3e(\pi)$ porphyrin orbitals, the splitting of the pyrrole-H resonance of the $\alpha\alpha\beta\beta$ atropisomer is consistent with preferential delocalization of unpaired electron spin into one of the two $3e(\pi)$ orbitals, due to the parallel alignment of the axial ligand planes.

The factors that affect the magnitudes of the contact shifts of low-spin ferric porphyrins in high-symmetry synthetic compounds,[2,3] simple natural hemins,[2,4] and heme proteins[5-11] have been investigated in detail for some time. NMR studies[2,3] have shown that unpaired spin delocalization takes place mainly to the pyrrole positions, which implicates the filled $3e(\pi)$ molecular orbitals[12] of the porphyrin in ligand-to-metal $\pi$ back-bonding to the remaining hole in the $d_{xz}$, $d_{yz}$ orbitals of iron.[2-4] The experimental observation of large contact shifts at the pyrrole positions has led to the wide utility of NMR spectroscopy, particularly in studies of groups appended to the pyrrole positions, in understanding the physical and chemical properties of a variety of heme proteins.[5-11] An important aspect of recent NMR investigations of low-spin ferric porphyrins[2-4,17,18] has been the attempt to explain the variation in the methyl resonance pattern of hemoproteins containing the common prosthetic group iron(III) protoporphyrin IX.[8,10,11]

One hypothesis[2,6] that has been advanced to explain the variation in methyl contact shifts in the heme proteins is that planar axial ligands lift the degeneracy of the $3e(\pi)$ filled molecular orbitals of the porphyrin ring and the e-symmetry $d_{xz}$, $d_{yz}$ orbitals of the metal; thus unpaired electron delocalization to certain pyrrole positions would be favored over others. The presence of one planar axial ligand, e.g., imidazole, whose freedom to rotate has been restricted, should be sufficient to lift the degeneracy of the $3e(\pi)$ and $d_\pi$ orbitals. Such restriction in the free rotation is expected to occur in hemoglobins, myoblobins, the cytochromes, and other hemoproteins where the axial ligands are provided to the metal by side chains of the protein backbone. In the case of the imidazole group of the almost ubiquitous histidine, the axial ligand is often stabilized in its angular orientation by hydrogen bonds between the imidazole N–H proton and the protein backbone.[13-16] Two planar axial ligands, as are present in the cytochromes $b_5$[15] and $b_2$[10] (two histidine imidazoles), should lift the degeneracy of the $3e(\pi)$ and $d_\pi$ orbitals unless their axial ligand planes are perpendicular. (In the solid-state structure of cytochrome $b_5$ they are known to be nearly coplanar,[15] or "parallel" in our terminology.)

It is possible that the alignment of axial ligand planes is used by nature to tune such important properties as the redox potentials of the cytochromes or the stability of the iron–dioxygen bond in hemoglobins. The testing of this hypothesis by use of simple model compounds is the goal of this series of investigations.

Two recent studies of model systems[17,1] have attempted to show the importance of restricted rotation of an axial ligand in splitting the metal $d_\pi$ and porphyrin $e(\pi)$ orbitals. In both cases, the systems studied contained unsymmetrically substituted porphyrin rings. Thus it was difficult to separate substituent effects from fixed axial ligand plane effects, since substituent effects alone can greatly perturb the pattern of unpaired electron delocalization into the porphyrin $\pi$ orbitals.[19]

† San Francisco State University.
‡ University of California.

(1) Recipient, NIH Research Career Development Award, 1976–1981.
(2) LaMar, G. N.; Walker, F. A. In "The Porphyrins"; Dolphin, D., Ed.; Academic Press: New York, 1979; Vol IV, pp 61–157 and references therein.
(3) LaMar, G. N.; Walker, F. A. *J. Am. Chem. Soc.*, **1973**, *95*, 1782–1790.
(4) LaMar, G. N.; Bold, T. J.; Satterlee, J. D., *Biochim. Biophys. Acta* **1977**, *498*, 189–207. LaMar, T. N.; DeGaudio, T. J.; Frye, J. S. *Ibid.* **1977**, 422–435, 499. LaMar, G. N.; Viscio, D. B.; Smith, K. M.; Caughey, W. S.; Smith, M. L. *J. Am. Chem. Soc.* **1978**, *100*, 8085–8092.
(5) Kowalsky, A. *Biochemistry*, **1965**, *4*, 2382–2388. Wuthrich, K. *Struct. Bonding (Berlin)*, **1970**, *8*, 53–121.
(6) Shulman, R. g.; Glarum, S. H.; Karplus, M. *J. Mol. Biol.* **1971**, *57*, 93–115.
(7) Mayer, A.; Ogawa, S.; Shulman, R. G.; Yamane, T.; Cavaleiro, J. A. S.; Rocha Gonsalves, A. M. d'A.; Kenner, G. W.; Smith, K. M. *J. Mol. Biol.* **1974**, *86*, 749–756.
(8) LaMar, G. N.; Overkamp, M.; Sick, H.; Gersonde, K., *Biochemistry*, **1978**, *17*, 352–361. LaMar, G. N.; Viscio, D. B.; Gersonde, K.; Sick, H. *Ibid.* **1978**, *17*, 361–367.
(9) Keller, R. M.; Wuthrich, K., *Biochim. Biophys. Acta* **1972**, *285*, 326–336. Keller, R.; Groudinsky, O.; Wuthrich, K. *Ibid.* **1973**, *328*, 233–238. Keller, R.; Groudinsky, O.; Wuthrich, K. *Ibid.* **1976**, *427*, 497–511. Keller, R.; Wuthrich, K. *Ibid.* **1980**, *621*, 204–217.
(10) Chao, Y.-Y. H.; Bersohn, R.; Aisen, P. *Biochemistry* **1979**, *18*, 774–779.
(11) LaMar, G. N.; Burns, P. D.; Jackson, J. T.; Smith, K. M.; Langry, K. C.; Strittmatter, P. *J. Biol. Chem.* **1981**, *256*, 6075–6079.
(12) Longuet-Higgins, H. C.; Rector, C. W.; Platt, J. R. *J. Chem. Phys.* **1950**, *18*, 1174–1181.
(13) Quiocho, F. A.; Lipscomb, W. N. *Adv. Protein Chem.* **1971**, *25*, 1–49.
(14) Richardson, J. S.; Thomas, K. A.; Rubin, B. H.; Richardson, D. C. *Proc. Natl. Acad. Sci.* U.S.A., **1975**, *72*, 1349–1353.
(15) Mathews, F. S.; Argos, P.; Levine, M., *Cole Spring Harbor Symp. Quant. Biol.*, **1971**, *No. 36*, 387–395. Mathews, F. S.; Cdzerwinski, E. W.; Argos, P. In "The Porphyrins"; Dolphin, D., Ed.; Academic Press: New York, 1979; Vol. VII, pp 107–147. Mathews, F. S. *Biochim. Biophys. Acta* **1980**, *622*, 375–379.
(16) Timkovich, R. In "The Porphyrins"; Dolphin, D., Ed.; Acadmic Press: New York, 1979; Vol. VII, pp 241–294.
(17) Traylor, T. G.; Berzinis, A. P. *J. Am. Chem. Soc.* **1980**, *102*, 2844–2846.
(18) Walker, F. A. *J. Am. Chem. Soc.* **1980**, *102*, 3254–3256.

0002-7863/83/1505-6923$01.50/0 

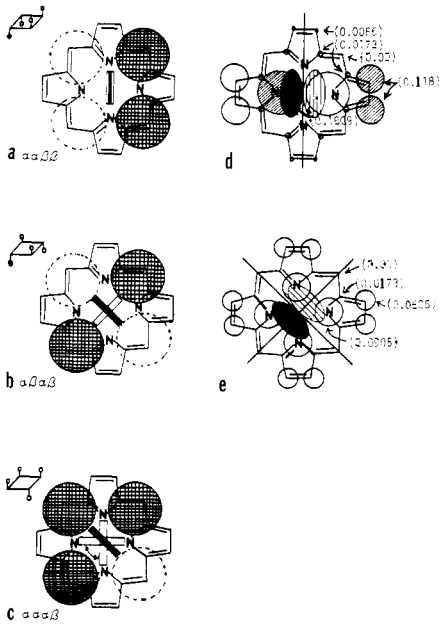

**Figure 1.** (a–c) Schematic representation of the arrangement of bulky *o*-pivalamido groups above ($\alpha$, cross-hatched circles) and below ($\beta$, dotted circles) the porphyrin plane and the expected orientation of axial ligand planes (above-the-plane ligand, solid rectangle, and below-the-plane ligand, open rectangle), for (a) $\alpha\alpha\beta\beta$ and (b) $\alpha\beta\alpha\beta$ atropisomers. In part c, the $\alpha\alpha\alpha\beta$ isomer, believed to have been formed during metal insertion (see text), the possible rotation of the below-the-plane ligand is indicated, and one of several possible unfavorable, short-lived orientations of the above-the-plane ligand is shown. (d, e) The expected electron density distributions in the 3e($\pi$) porphyrin molecular orbital which interacts with low-spin Fe(III). The orbital of part d is one of a pair, the other member of which has its nodal plane oriented at 90° to that shown. Part e represents the average of the two orbitals of part d, or equivalently, their linear combinations which have nodal planes passing through the meso carbons.[18] The supposition of this work is that the nodal plane of the imidazole ligands will lie in the nodal planes of the 3e($\pi$) orbitals in the two limiting geometries imposed by the bulky groups of parts a and b. The molecular orbital coefficients, $c_1^2$, which are proportional to the electron density at each position,[12] are included in parentheses in parts d and e. The $\pi$ orbitals of the *N*-methylimidazole are included in part d and that of the upper *N*-MeIm is included in part e.

We wish to report the preparation and NMR investigation of symmetrically substituted tetraphenylporphyrin isomers designed in such a way as to restrict the rotation of planar axial ligands and hold them either parallel or perpendicular to each other. The method we have used to restrict the rotation of planar axial ligand is to use a bulky substituent on one ortho position of each phenyl group of tetraphenylporphyrin, in order to eliminate the unsymmetrical substituent effect,[19] and to arrange the ortho substituents above ($\alpha$) and below ($\beta$) the porphyrin plane in geometrical arrangements that will lead to the two extreme orientations of the axial imidazoles by crowding them into parallel and perpendicular orientations. This situation is shown in Figure 1a,b, where circles denote bulky ortho substituents. Our initial studies have focused upon two of the atropisomers of tetrakis(*o*-pivalamidophenyl)porphyrin, of which the $\alpha\alpha\alpha\alpha$ atropisomer (not shown in Figure 1) is known as the picket fence porphyrin.[20] The two isomers of interest are the $\alpha\alpha\beta\beta$ isomer, Figure 1a, which is expected to hold the axial imidazoles parallel, and the $\alpha\beta\alpha\beta$ isomer, Figure 1b, which should hold them in perpendicular planes. The results of this study clearly show that in the absence of substituent effects, an axial ligand plane is capable of lifting the degeneracy of the metal $d_\pi$ and porphyrin e($\pi$) orbitals. It also points out some of the complicating features of the *o*-pivalamido substituent with regard to this particular study.

## Experimental Section

**Materials and Methods.** Pyrrole, *o*-nitrobenzaldehyde, pyridine, *N*-methylimidazole, and pivaloyl chloride were purchased from Aldrich. Deuteriochloroform was a product of Norell Chemical Co. Solvents (reagent grade THF, methylene chloride, ethyl acetate, methanol, chloroform) were products of Fisher Scientific Co. $FeBr_2$ and $SnCl_2$ were purchased from Alfa.

Pyrrole and *N*-methylimidazole were distilled before use. Pyridine was distilled from sodium and THF from sodium and benzophenone under argon immediately before use. Other reagents and solvents were used as received.

Thin layer chromatography was carried out with Eastman Chromagram silica gel plates. Gravity flow column chromatography was done with Baker 3405 silica gel (60–200 mesh). Medium-pressure liquid chromatography (MPLC) was also tried by using E. M. Reagents silica gel 60 (230–400 mesh), with columns and tubing made by Altex. Solvent flow rate was controlled with a pump made by Fluid Metering, Inc., and the effluent was monitored on a Beckman UV detector.

Routine NMR spectra were recorded on a Varian EM-360 NMR spectrometer. High-field (200 MHz) spectra were run on the NMR spectrometer in the Chemistry Department at the University of California, Berkeley. Electronic absorption spectra were recorded on Perkin-Elmer 552 and Cary 17 UV-visible spectrophotometers.

**Preparation of Compounds.** *meso*-Tetrakis(*o*-nitrophenyl)porphyrin ($(o\text{-}NO_2)_4TPPH_2$) was prepared by published procedures[20,21] and purified by gravity column chromatography on silica gel with methylene chloride to elute the unseparated atropisomers. This mixture of atropisomers was reduced to the same mixture of atropisomers of *meso*-tetrakis(*o*-aminophenyl)porphyrin ($(o\text{-}NH_2)TPPH_2$) by the $SnCl_2$/HCl method of Collman and co-workers.[20] Since the atropisomer desired by these workers ($\alpha\alpha\alpha\alpha$) is the most polar of the four, different chromatographic procedures had to be developed to separate the less polar and more similar in retention time atropisomers, $\alpha\beta\alpha\beta$ and $\alpha\alpha\beta\beta$. The best method found was to pack a 4-cm diameter gravity column with a slurry of silica gel in methylene chloride to a height of about 125 cm, top the column with 1–2 cm sand, and introduce ca. 500 mg of $(o\text{-}NH_2)_4TPPH_2$ as a saturated, filtered solution in $CH_2Cl_2$ (approximately 100-mL total volume of solution). The column was then washed with 1 L of $CH_2Cl_2$ to remove nonpolar impurities, and then the desired $\alpha\beta\alpha\beta$ (band 1) and $\alpha\alpha\beta\beta$ (band 2) atropisomers were eluted with a mixture of $CH_2Cl_2$ and small amounts of ethyl acetate, usually 5%, but gradient elutions of 5–50% ethyl acetate were also tried. Complete separation of significant quantities of the two atropisomers, which have similar retention times ($R_f$ $\alpha\beta\alpha\beta$ 0.77, $\alpha\alpha\beta\beta$ 0.64, silica gel, 1:1 benzene–ether[20]), was, however, difficult to achieve and time consuming, especially in view of the slow rotational isomerization of each of the separated isomers to the $\alpha\alpha\alpha\beta$ atropisomer. MPLC also did not produce sufficient quantities of pure atropisomers to permit the desired iron porphyrin NMR studies to be carried out. Similar studies of the *o*-pivalamidophenyl atropisomers discussed below also indicated that pure isomers could be separated in only small quantities. Thus it was decided to pursue the goals of the project by using quantitated mixtures of the two isomers, which could be obtained in sufficient quantity in relatively short times (2–4 h). In obtaining these quantitated mixtures of isomers, gradient elution (5–50% ethyl acetate in $CH_2Cl_2$) of the two bands was used. Different portions of the mixed isomers "band" were selected in each separation, and the ratio $\alpha\beta\alpha\beta$:$\alpha\alpha\beta\beta$ was determined by methods described below.

In order to minimize rotation of the aminophenyl groups of the $\alpha\beta\alpha\beta$ and $\alpha\alpha\beta\beta$ atropisomers of $(o\text{-}NH_2)_4TPPH_2$, once separated from the others, they were reacted immediately (in the receiving flask) with pivaloyl chloride: 20 mL of $CH_2Cl_2$, 3 mL of (pivaloyl) chloride ($2 \times 10^{-2}$ mol), and 3 mL of pyridine were placed in the receiving flask in which the column eluent of the mixture of these two atropisomers was collected. Approximately 500 mL, estimated to contain ca. 50 mg, or $7 \times 10^{-5}$ mol of $(o\text{-}NH_2)_4TPPH_2$ was thus collected and reacted with pivaloyl chloride in each preparation. The resulting solutions were stirred for 2–3 h and then evaporated at reduced temperature and pressure. All procedures, including column chromatography, amide formation, evaporation, and subsequent procedures described below, were carried out under subdued room light or in light-protected containers to prevent photoatropisomerization.[22]

The crude tetrakis(*o*-pivalamidophenyl)porphyrin ($(o\text{-piv})_4TPPH_2$) obtained by the above procedures was dissolved in $CH_2Cl_2$ and washed 3 times with dilute aqueous NaOH, once with water, and finally with aqueous NaCl. After volume reduction of the organic phase, the product

(19) Walker, F. A.; Balke, V. L.; McDermott, G. A. *J. Am. Chem. Soc.* **1982**, *104*, 1569–1574.
(20) Collman, J. P.; Gagne, R. R.; Reed, C. A.; Halbert, T. R.; Lang, G.; Robinson, W. T. *J. Am. Chem. Soc.* **1975**, *97*, 1427–1439.
(21) Adler, A. D.; Longo, F. R.; Finarelli, J. O.; Goldmacher, J.; Assour, J.; Morsakoff *J. Org. Chem.* **1967**, *32*, 476.
(22) Freitag, R. A.; Mercer-Smith, J. A.; Whitten, D. G. *J. Am. Chem. Soc.* **1981**, *103*, 1226–1228.

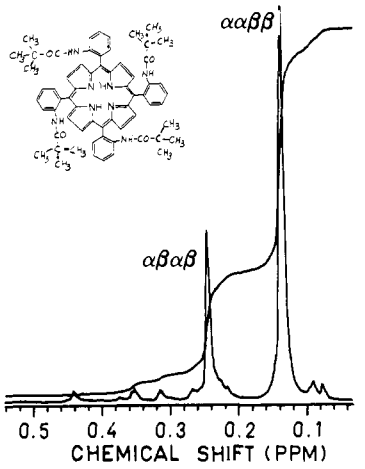


**Figure 2.** Proton NMR spectrum (200 MHz) of the pivalamido methyl region of a sample of ((*o*-piv)$_4$TPP)H$_2$ which, from TLC spot intensities, appeared to have a ratio of $\alpha\beta\alpha\beta$:$\alpha\alpha\beta\beta$ atropisomers of ca. 1:2. Integrated intensities and peak heights both place this ratio at 1:2.3. This sample was later used to prepare Fe(III)-containing sample II.

Table I. Proton NMR Shifts of Free-Base Atropisomers of ((*o*-piv)$_4$TPP)H$_2$[a]

| proton type | total integrated intensity (both isomers) | chemical shifts, ppm from Me$_4$Si[a] $\alpha\beta\alpha\beta$ | $\alpha\alpha\beta\beta$ |
|---|---|---|---|
| pyrrole H | 8 | 8.83 (s) | 8.85 (s) |
| phenyl H | | | |
| ortho | 4 | 8.69 (d, $J$ = 9 Hz)[b] | 8.74 (d, $J$ = 9 Hz)[b] |
| meta | 8 | 7.87 (m, $J$ = 9 Hz)[b] | 7.87 (m, $J$ = 9 Hz)[b] |
| para | 4 | 7.51 (t, $J$ = 9 Hz)[b] | 7.51 (t, $J$ = 9 Hz)[b] |
| amide N-H | 4 | 7.22 (s) | 7.17 (s) |
| piv(Me) H | 36 | 0.24 (s) | 0.13 (s) |
| porphyrin N-H | 2 | −2.64 (s) | −2.64 (s) |

[a] Recorded at 200 MHz in $CDCl_3$. [b] d = doublet; m = multiplet; t = triplet.

was purified by column chromatography using methylene chloride–ethyl acetate gradient elution. The methods used to monitor the purification of the (*o*-piv)$_4$TPPH$_2$ samples were electronic absorption spectrophotometry, TLC, and NMR spectrometry. Visible spectral peaks used (solvent = $CH_2Cl_2$) were those at 650, 590, 545, 515, and 485 (sh) nm. The quantity of $\alpha\beta\alpha\beta$:$\alpha\alpha\beta\beta$ was determined from the integrated intensities of the methyl proton resonances at 0.25 ppm ($\alpha\beta\alpha\beta$) and 0.13 ppm ($\alpha\alpha\beta\beta$), following rough estimation from the intensity of the TLC spots, as illustrated in Figure 2. $Me_4Si$ was not added to the $CDCl_3$ solutions; thus chemical shifts have been calculated on the basis of the $CHCl_3$ proton resonance position (7.25 ppm). Proton NMR assignments of all resonances of each isomer are presented in Table I.

Insertion of iron into the quantitated mixtures of $\alpha\beta\alpha\beta$ and $\alpha\alpha\beta\beta$ (*o*-piv)$_4$TPPH$_2$ was accomplished by modification of the method of Collman et al:[23] (*o*-piv)$_4$TPPH$_2$ (40 mg), pyridine (1 mL), and anhydrous $FeBr_2$ (100 mg) were refluxed in dry THF (40 mL) under argon. The progress of metal insertion was monitored by withdrawing small aliquots and measuring their electronic absorption spectrum, particularly the loss of the peak at 650 nm. No care was taken to exclude oxygen from cuvettes, and thus the metalloporphyrin peaks observed as the metal insertion progressed were those of the Fe(III) bromide porphyrin (major peaks at 510 and 585 nm). Metal insertion was judged complete after ca. 2.5–3 h. The solvent was then evaporated, with no further precautions taken to exclude oxygen, and the residue was chromatographed on silica gel with 1:1 methylene chloride/ethyl acetate to remove any metal-free (*o*-piv)$_4$TPPH$_2$, and then with 10% methanol in $CHCl_3$. Two bands were observed [probably ((*o*-piv)$_4$TPF)FeBr and ((*o*-piv)$_4$TPP)FeOH], but were combined and evaporated to dryness. The sample was redissolved in methylene chloride, and HCl gas was then bubbled through the solution, followed by evaporation to dryness. At this point the sample of atropisomers of ((*o*-piv)$_4$TPP)FeCl was homogeneous to TLC; only one spot was observed, independent of the mixture of solvents (methylene chloride/ethyl acetate or chloroform/methanol) used as the moving phase.

In several cases ion exchange was carried out by methods described previously[24] to produce the iodoiron derivatives of ((*p*-piv)$_4$TPP)FeI.

NMR spectra were obtained in $CDCl_3$ for the free base (Table I, Figure 2) and Fe(III) complexes of three samples, hereafter called I, II, and III, which were prepared from 1:1, 1:2.3, and 1:2.9 ratios of $\alpha\beta\alpha\beta$:$\alpha\alpha\beta\beta$ metal-free atropisomers, respectively. The Fe(III) samples I–III were investigated in their high-spin (HS) chloroiron(III) and low-spin (LS) bis(*N*-methylimidazole) (*N*-MeIm) complex forms. The *N*-MeIm concentration dependence of each sample was investigated by adding successive aliquots of *N*-MeIm to each NMR tube.

## Results and Discussion

**NMR Spectra of the Metal-Free $\alpha\beta\alpha\beta$ and $\alpha\alpha\beta\beta$ Atropisomers.** Although they were not separated in large enough quantity to allow NMR investigation of the atropisomers separately, it was possible to assign the individual NMR resonances of the $\alpha\beta\alpha\beta$ and $\alpha\alpha\beta\beta$ atropisomers. Since the relative retention times of the $\alpha\beta\alpha\beta$ and $\alpha\alpha\beta\beta$ atropisomers are known,[20] the approximate desired ratio of atropisomers could be predetermined by cutting off either the beginning or the end of the mixture of the two bands. Testing the flask of eluate by TLC then allowed a check of the approximate ratio of atropisomers actually obtained. The relative intensities of the two proton NMR resonances near 0 ppm, in comparison to the estimated approximate ratios of $\alpha\beta\alpha\beta$ to $\alpha\alpha\beta\beta$ obtained from the intensity of TLC spots, then allowed assignment of the methyl peak of the pivalamido group of the $\alpha\beta\alpha\beta$ (0.25 ppm) and $\alpha\alpha\beta\beta$ (0.13 ppm) isomers. A minor peak present at 0.09 ppm is believed to be due to the picket fence ($\alpha\alpha\alpha\alpha$) isomer on the basis of previous reports[20] and our own studies of peak growth upon refluxing, and two peaks near 0.22 ppm plus one at 0.15 ppm are believed to be due to the $\alpha\alpha\alpha\beta$ isomer, on the basis of the growth of these peaks upon refluxing a sample for 8 h in toluene. [Both $\alpha\beta\alpha\beta$ and $\alpha\alpha\beta\beta$ atropisomerize to $\alpha\alpha\alpha\beta$ upon rotation of a single phenyl group.] the nature of the other minor peaks in the 0–1 ppm range is not known, but they are nonporphyrinic, on the basis of comparison with the integrated intensity of this region to that of the aromatic region (7–10 ppm).

The slight difference in chemical shifts for the $\alpha\beta\alpha\beta$ and $\alpha\alpha\beta\beta$ atropisomers of the pivalamido methyl and NH protons, which are inside the "ring", is indicative of slightly smaller ring current shifts for the $\alpha\beta\alpha\beta$ isomer. The two isomers are probably differently solvated, as suggested in previous NMR studies of ((*o*-$CH_3$)$_4$TPP)Ni.[25]

Refluxing mixtures of known ratios of $\alpha\beta\alpha\beta$ to $\alpha\alpha\beta\beta$ (*o*-piv)$_4$TPPH$_2$ for long periods of time in toluene (bp 111 °C) caused rotation of the pivalamidophenyl groups. After 8 h in refluxing toluene, a sample mixture having an initial isomer ratio of 1:3.9 was found to connain an approximate ratio of 1:4:3.8:0.27 $\alpha\beta\alpha\beta$:$\alpha\alpha\beta\beta$:$\alpha\alpha\alpha\beta$:$\alpha\alpha\alpha\alpha$, or ca. 42% of the original sample had been converted into the $\alpha\alpha\alpha\beta$ atropisomer and 3% into the $\alpha\alpha\alpha\alpha$, on the basis of NMR peak intensities. These observed isomer ratios after 8 h of reflux are not in line with those predicted if the final equilibrium ratio is to be 1:2:4:1, as expected statistically or as observed for ((*o*-$CH_3$)$_4$TPP)Ni[25] and (*o*-OH)$_4$TPPH$_2$,[26] but is more in line with the observed isomer distribution in (*o*-CN)$_4$TPPH$_2$.[27] Thus both seric effects of bulky substituents and electronic effects of electron-rich substituents[27] may influence the equilibrium ratio of the four atropisomers to be different from that expected on statistical grounds.

(23) Collman, J. P.; Brauman, J. I.; Doxsee, K. M.; Halbert, T. R.; Bunnenberg, E.; Linder, R. E.; LaMar, G. N.; DelGaudio, J.; Lang, G.; Spartalian, K. *J. Am. Chem. Soc.* **1980**, *102*, 4182–4192.

(24) Walker, F. A.; LaMar, G. N. *Ann. N. Y. Acad. Sci.* **1973**, *206*, 328–348.

(25) Walker, F. A.; Avery, G. L. *Tetrahedron* Lett. **1971**, 4949–4952.

(26) Gottwald, L. K.; Ullman, E. F. *Tetrahedron Lett.*, **1969**, 3071–3074.

(27) Hatano, K.; Anzai, K.; Kubo, T.; Tami, S. *Bull. Chem. Soc. Jpn.*, **1981**, *54*, 3518–3521.

Table II. Chemical Shifts of High-Spin Fe(III) Samples of the Atropisomers of ((o-piv)$_4$TPP)FeCl[a]

| sample (expected ratio $\alpha\alpha\beta\beta$:$\alpha\beta\alpha\beta$) | temp, °C | pyrrole H | phenyl H meta[b] | phenyl H para | -C(CH$_3$)$_3$ |
|---|---|---|---|---|---|
| I (1) | 21 | 81 | 12.1, 15.1 (70%); 13.4, 13.6 (30%) | 8.1 | −3[c] |
| II (2.3) | 21 | 81 | 12.1, 15.2 (66%); 13.4, 13.7 (34%) | 8.1 | −3[c] |
| III (2.9) | 21 | 81 | 12.1, 15.1 (~66%); 13.3, 13.6 (~34%) | 8.1 | −3[c] |
| ($\alpha\alpha\alpha\alpha$-(o-piv)$_4$TPP)FeBr[d] | 25 | | 12.5, 16.5[d] | | |
| II (mono(imidazole) complex)[e] | 21 | 79 | 10.8, 13.5 (~70%); 11.7, 12.2 (~30%) | | −2.5[c] |
| (TPP)FeCl[f] | 21 | 81 | 12.6, 13.7 | 7.9 | |
| (TPP)FeCl[g] | 21 | 81.3 | 12.3, 13.5 | 6.4 | |
| ((p-CH$_3$)$_4$TPP)FeCl[f] | 21 | 81 | 12.8, 13.8 | | |

[a] Recorded at 200 MHz in $CDCl_3$, with $Me_4Si$ as reference. [b] Two doublets observed (relative intensity in parenthesis). [c] Second resonance expected near 0 ppm, but not observed due to the presence of diamagnetic impurities. [d] Reference 30. [e] Observed when [N-MeIm] < 0.1 M. [f] Included for comparison. [g] Taken from ref 29.

**Metal Insertion.** Insertion of iron into the mixtures of the two isomers proved more difficult than suggested by the procedures reported for the picket fence porphyrin,[20,23] perhaps because the bulky pivalamido groups of the $\alpha\beta\alpha\beta$ and $\alpha\alpha\beta\beta$ atropisomers occur on both sides of the porphyrin plane and may thereby effectively hinder the approach of the metal ion. Heating times of ca. 2.5–3 h of the porphyrin under an argon atmosphere with $FeBr_2$ and a trace of pyridine in dry THF as solvent[23] were required to achieve metal insertion. This extended heating caused some rotation (atropisomerization) of pivalamidophenyl groups, as expected on the basis of the toluene reflux experiment of the free base atropisomers discussed above. However, the lower boiling point of THF (67 °C) and shorter reflux times were expected to cause considerably less atropisomerization. Unfortunately this expectation was not borne out in fact, as is discussed in detail below.

Exposure of the above reaction mixture to air caused oxidation of the iron. Isolation and chromatography of the ferric porphyrin samples[19] follwed by treatment with dry HCl gas and evaporation to dryness yielded the desired ((o-piv)$_4$TPP)FeCl forms of the mixed atropisomers. At this point, the polarity of the complexes is dominated not by the o-pivalamido groups, but rather by the weak $Fe^{III}Cl^-$ bond, and thus the atropisomeric Fe(III) complexes have identical retention times, as pointed out in the Experimental Section.

**NMR Spectra of the Mixed Atropisomeric High-Spin Samples of ((o-piv)$_4$TPP)FeCl.** In Figure 3 is shown the 200-MHz proton NMR spectrum of a 0.01 M solution of sample I, which was prepared from a 1:1 atropisomeric ratio of $\alpha\beta\alpha\beta$ to $\alpha\alpha\beta\beta$. Consistent with previous studies of high-spin $Fe^{III}$(TPP)s, the pyrrole H resonance is about 80 ppm downfield from $Me_4Si$ (relative intensity 8), the phenyl m-H resonances are centered at about 13 ppm downfield from $Me_4Si$ (total relative intensity 8), while the p-H resonance is slightly downfield from $CHCl_3$, at about 8 ppm (relative intensity 4). The phenyl o-H resonances (expected relative intensity 4) are located under the $CHCl_3$ peak, but are too broad to detect in Figure 3. Exact chemical shifts are given in Table II. The location of the p-H resonance position was confirmed by converting anions from $Cl^-$ to $I^-$, since p-H is known to appear ca. 1 ppm further downfield for the iodo complex.[28,29]

It should be noted that the p-H resonance is considerably downfield (1.7 ppm) from that of (TPP)FeCl,[28,29] as shown in Table II. The same is also true, but a lesser extent (0.7 ppm), for the average m-H resonance position of the atropisomers of ((o-piv)$_4$TPP)FeCl. Since all HS Fe(III) phenyl H dipolar shifts are downfield, while contact shifts alternate, with p-H upfield and m-H downfield,[28,29] it appears that the differences observed must be due to differences in the magnitudes of both the dipolar and contact contributions.

The breadth and relative intensity (14–16) of the signal at −3 ppm confirm that this signal is due to approximately half of the pivalamido methyl protons. The other pivalamido methyl peak is presumably hidden under the intense resonances of the 0–5 ppm region. Resonances in that region (except $Me_4Si$) are due to hydrocarbon impurities presumably introduced during insertion of iron and/or subsequent workup. These impurity resonances apparently mask the NH resonances. Also included in Table II are the chemical shifts of the pyrrole H, m-H, and pivalamido methyl H resonances of the "picket fence" porphyrin ($\alpha\alpha\alpha\alpha$) isomer of ((o-piv)$_4$TPP)FeBr[30] and those of the mono(N-methylimidazole) complex of ((o-piv)$_4$TPP)$Fe^{III}$, discussed below.

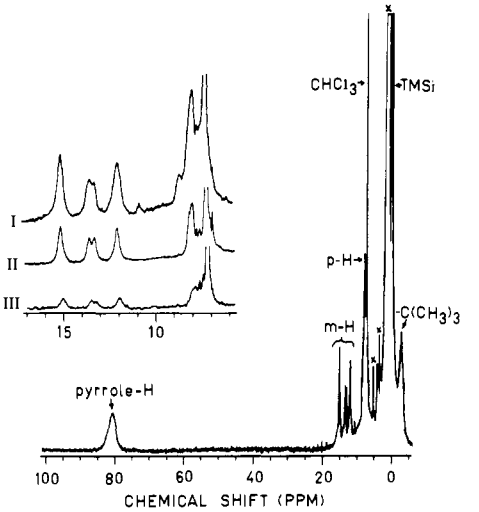


**Figure 3.** Proton NMR spectrum (200 MHz) of the high-spin chloroiron(III) form of sample I ($\alpha\beta\alpha\beta$:$\alpha\alpha\beta\beta$ = 1:1). Insert: Expansion of the 6–16 ppm region of samples I (1:1), II (1:2.3), and III (1:2.9). The integrated intensities of the downfield: center pair:upfield m-H signals are as follows: I (0.35:0.30:0.35), II (0.33:0.34:0.33), III (~0.33:~0.34:~0.33). Temperature = 21 °C, iron porphyrin concentration ca. 0.01 M or less in all spectra.

The insert of Figure 3 shows an expansion of the 6–17 ppm region of the spectrum of sample I. The same region of the spectra of samples II and III are also shown for comparison. The spectra of all samples are identical over the entire spectral range except for the minor differences in the intensity ratio of the phenyl m-H proton resonances located between 12 and 15 ppm, as shown in the insert. The major difference between the ((o-piv)$_4$TPP)FeCl samples shown in Figure 3 and those of previously studied (TPP)FeX derivatives, including the $\alpha\alpha\alpha\alpha$ isomer of ((o-piv)$_4$TPP)FeBr,[30] is the existence of four, rather than two, m-H resonances.

In previous studies of (TPP)FeCl,[2,24,28,29] its o-, m-, and p-tolyl analogues,[2,24,28] and halide[2,24,28,29] or pseudohalide[29] derivatives, two m-H (or m-$CH_3$) signals have always been observed. When the temperature[24] is raised or excess halide is added, these two signals can be caused to coalesce, when recorded at 100 MHz or below. The existence of two m-H resonances has been explained in terms of the out-of-plane position of Fe(III), which places the

(28) LaMar, G. N.; Eaton, G. R.; Holm, R. H.; Walker, F. A. *J. Am. Chem. Soc.* **1973**, *95*, 63–75.
(29) Behere, D. V.; Birdy, R.; Mitra, S. *Inorg. Chem.* **1982**, *21*, 386–390.
(30) Latos-Grazynski, L.; LaMar, G. N.; Balch, A. L., submitted for publication.

two phenyl *m*-H protons at different distances and angles from the paramagnetic center, thus leading to different dipolar shifts for the two *m*-H. (The same phenomenon is expected for the phenyl *o*-H proton resonances, but they are usually, though not always,[29,30] too broad to be resolved.) The protons can be made equivalent on the 100-MHz time scale through kinetic processes (increasing the rate of phenyl rotation[24] or increasing the rate of halide exchange and thus "iron inversion"[31]).

In each of the spectra (of samples I–III) shown in the insert of Figure 3, the four *m*-H resonances appear as two pairs of equal intensity peaks, one located at 12.1 and 15.1 ppm and the other at 13.3 and 13.6 ppm. The outer pair are located in very similar positions to the two *m*-H resonances observed for $\alpha\alpha\alpha\alpha$-((*o*-piv)$_4$TPP)FeBr[30] (Table II). What difference there is in chemical shift is attributable to the change in counterion from chloride to bromide.[2,28] The two pairs are of roughly the same intensity ratio for all three samples (ranging from 30% inner, 70% outer for sample I to 34% inner, 66% outer for sample II, and about the same for sample III). Thus it is clear that the intensity ratio of the inner and outer pairs of *m*-H peaks is not indicative of the ratio of $\alpha\beta\alpha\beta$ to $\alpha\alpha\beta\beta$ atropisomers. Rather, we believe that it is indicative of the degree of atropisomerization (phenyl rotation) during metal insertion. Assuming that the two (inequivalent) *m*-H of an *o*-pivalamidophenyl group will have different dipolar shifts depending on whether the *o*-pivalamido group is on the same side as the halide or the opposite side, then the $\alpha\alpha\beta\beta$ and $\alpha\beta\alpha\beta$ atropisomers should each have four *m*-H signals of equal intensity and the $\alpha\alpha\alpha\beta$ atropisomer should have two *m*-H signals of relative intensity 3 and two of relative intensity 1. It is reasonable to expect that the two signals of relative intensity 3 should be in the same positions as the two signals observed for the $\alpha\alpha\alpha\alpha$ isomer. This corresponds to assuming that the $\alpha\alpha\alpha\alpha$ and $\alpha\alpha\alpha\beta$ atropisomers have the halide bound preferentially on one side. (Which side is not important to the present discussion, though it would appear to be the "$\beta$" side.) However, for the $\alpha\alpha\beta\beta$ and $\alpha\beta\alpha\beta$ isomers there is no preferred side. If the samples I–III of the insert of Figure 3 contained only the desired $\alpha\alpha\beta\beta$ and $\alpha\beta\alpha\beta$ atropisomers, then four equal-intensity *m*-H signals would be observed. However, since the outer peaks are about twice as intense as the inner, there must be significant amounts of $\alpha\alpha\alpha\beta$ (and probably also $\alpha\alpha\alpha\alpha$) isomer present. Rough estimates suggest that all three samples (I–III, insert, Figure 3) contain between 45 and 55% of the undesired isomers, depending on the relative amounts of $\alpha\alpha\alpha\beta$ and $\alpha\alpha\alpha\alpha$ assumed present. Thus the excess intensity in the outer *m*-H peaks is indicative of extensive and similar amounts of atropisomerization during metal insertion. In fact, approximately the same percentage of atropisomerization was apparently achieved through refluxing the free base in toluene at 111 °C for 8 h as through reluxing the free base in THF in the presence of $FeBr_2$ and pyridine at 67 °C for 2.5–3 h. The metal ion probably catalyzes atropisomerization by distorting the porphyrin ring from planarity during metal insertion. In view of our experience, it is remarkable that the iron complex of the picket fence porphyrin ($\alpha\alpha\alpha\alpha$) can be obtained atropisomerically pure. However, the shorter reaction time for metal insertion,[20] as well as the fact that the less polar, more readily crystallizable Fe(II) form was isolated, in large enough quantity to permit recrystallization, undoubtedly greatly reduced the problem of atropisomeric contamination in the case of the picket fence porphyrin.

In spite of the atropisomerization reaction, it was possible to achieve our goal of demonstrating that axial ligand planes lift the degeneracy of the 3e($\pi$) orbitals of low-spin Fe(III), as is discussed below.

**NMR Studies of the Addition of *N*-Methylimidazole to the Mixed Atropisomeric Samples of ((*o*-piv)$_4$TPP)FeCl, and the Effect of Axial Ligand Plane Orientation.** As small aliquots of *N*-MeIm are added to the mixed atropisomers of ((*o*-piv)$_4$TPP)FeCl (ca. 0.05 M) in $CDCl_3$, the peaks due to the high-spin form decrease in intensity while peaks due to the low-spin form begin to appear, as shown in Figure 4. The most clearly

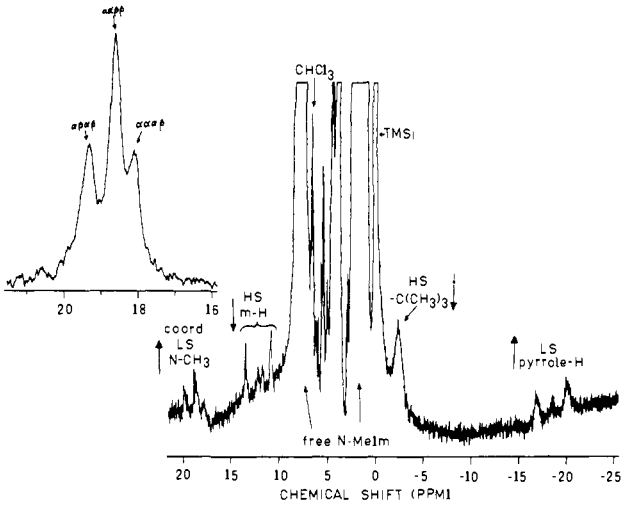


**Figure 4.** Proton NMR spectrum (200 MHz) of sample II (ca. 0.01 M) containing 0.05 M *N*-MeIm. (Temperature = 21 °C.) The peaks in the 17–20 ppm region are due to the $CH_3$ group of coordinated *N*-MeIm in the low-spin bis axially ligated form.[35] Those in the 10–14 ppm region are due to the phenyl *m*-H protons of remaining high-spin iron(III) porphyrin species, and since they are at different chemical shifts than those in Figure 3, they must be due to the 5-coordinate, high-spin atropisomers of ((*o*-piv)$_4$TPP)Fe(*N*-MeIm)$^+$Cl$^-$. The broad peak at −2.5 ppm is due to half of the pivalamido methyl groups of the high-spin, mono(*N*-MeIm) complex, while those between −16 and −21 ppm are due to the pyrrole H of the low-spin forms of the atropisomers of ((*o*-piv)$_4$TPP)Fe(*N*-MeIm)$_2^+$Cl$^-$. Insert: $CH_3$ region of coordinated *N*-MeIm of sample II when [*N*-MeIm] = 0.6 M.

diagnostic peak for low-spin Fe$^{III}$(TPP) complexes is the pyrrole H resonance,[2-4] which is found upfield from $Me_4Si$ at about −18 ppm for (TPP)Fe(*N*-MeIm)$_2^+$Cl$^-$ at 22 °C. At relatively low (<0.1 M) concentrations of *N*-MeIm, three pyrrole H resonances are evident in Figure 4, one at ca. −18.5 ppm, and two, of equal intensity, at ca. −17 and −20 ppm. As [*N*-MeIm] is increased to 0.1 M and above (Figure 5), two changes occur: (1) the ratio of central to combined outer peaks increases and, at 0.6 M *N*-MeIm and above, is very close to the ratio of $\alpha\beta\alpha\beta$:$\alpha\alpha\beta\beta$ atropisomers originally present in each free base sample;[32] and (2) a new peak appears at ca. −19.3 ppm and grows in intensity to ca. 25–30% of the total pyrrole proton intensity at [*N*-MeIm] = 0.6 M.[34] It continues to grow slowly above 0.6 M *N*-MeIm, but dynamic range problems, due to the intense proton resonances of the free ligand, limit the accuracy of measurements of peak areas. It is reasonable to aqssume that at sufficiently high [*N*-MeIm] its intensity will approach 40–50% of the total, as expected on the basis of the high-spin Fe(III) spectra discussed above. Thus the pyrrole proton peaks of the ((*o*-piv)$_4$TPP)Fe(*N*-MeIm)$_2^+$ samples of Figure 5 may be assigned as follows: $\alpha\beta\alpha\beta$, −18.6 ppm; $\alpha\alpha\beta\beta$, −17.1 and −20.0 ppm; $\alpha\alpha\alpha\beta$, −19.5 ppm at 21 °C.[34] We will return to a detailed discussion of these pyrrole H resonances following a short digression concerning several features of the spectrum shown in Figure 4, where the *N*-methylimidazole concentration is very low.

(31) Snyder, R. V.; LaMar, G. N. *J. Am. Chem. Soc.* **1976**, *98*, 4419.

(32) The concn. dependence of the intensity ratios of outer to outer to central peaks in Figure 5 indicates that the equilibrium constant, $\beta_2$, for addition of two *N*-methylimidazole ligands to the $\alpha\beta\alpha\beta$ isomer isomer is considerably smaller than that for the $\alpha\alpha\beta\beta$ isomer, as might well be expected on steric grounds. Rough (factor of 2) estimates of $\beta_2$ for the two isomers, based upon peak intensities, are 500 ($\alpha\alpha\beta\beta$) and 50 ($\alpha\beta\alpha\beta$) M$^{-2}$, respectively. These estimates may be compared to $\beta_2$ for addition of the same ligand to (TPP)FeCl (1500 M$^{-2}$).[32] The difference is attributable to a combination of electronic and steric effects, the latter probably mainly upon the constant for the second step, $K_2$.

(33) Walker, F. A.; Lo, M.-W.; Ree, M. T. *J. Am. Chem. Soc.* **1976**, *98*, 5552–5560.

(34) Recent work (G. A. McDermott and F. A. Walker, unpublished results) shows a similar fourth resonance in other sterically hindered complexes, including ((*o*-$C_6H_{13}$)$_4$TPP)Fe(*N*-MeIm)$_2$, but in this case it appears downfield from the central ($\alpha\beta\alpha\beta$ isomer) resonance, and the total spread of pyrrole H resonances is much smaller than that reported here.

In Figure 4, we note the appearance of three peaks in the 18–20 ppm region downfield from $Me_4Si$. These peaks grow in intensity as do the peaks upfield from $Me_4Si$ as the concentration of *N*-MeIm is increased. Their integrated intensity relative to the pyrrole H peaks is 6:8. They thus are due to the $CH_3$ protons of coordinated *N*-MeIm[35] of the three atropisomeric low-spin Fe(III) complexes. From their concentration dependence, which parallels that of the pyrrole H resonances, they may be assigned to the N–$CH_3$ protons of the bis(*N*-methylimidazole) complexes of the $\alpha\beta\alpha\beta$ (19.3 ppm), $\alpha\alpha\beta\beta$ (18.6 ppm), and $\alpha\alpha\alpha\beta$ (18.1 ppm) atropisomers.

It should also be noted (Figure 4) that at low [*N*-MeIm] the remaining signals from the *m*-H protons of the high-spin Fe(III) porphyrinic species still consist of four peaks, in the same intensity ratio (66% outer, 34% inner), but with their positions shifted somewhat upfield and their separations slightly changed (Table II). These results suggest (1) that the nature of the axial ligand, and thus probably both out-of-plane position and the zero-field splitting constant of Fe(III), has changed, presumably due to replacement of $Cl^-$ by one *N*-MeIm, and (2) that the stepwise equilibrium constant $K_1$, for addition of one *N*-MeIm, is fairly similar for all three atropisomers of ((*o*-piv)$_4$TPP)FeCl as well as to that for (TPP)FeCl ($\sim$150 $M^{-1}$),[33] but that $K_2$ is much smaller,[32] and thus we are able to observe the NMR spectrum of the mono(*N*-MeIm) complexes of ((*o*-piv)$_4$TPP)Fe(III). Observation of two pairs of *m*-H resonances for the mono(*N*-MeIm) complexes (Figure 4), as was also found for the chloro complex complex (Figure 3), establishes unambigously that Fe(III) is out of the porphyrin plane and thus the complexes exist as 5-coordinate ion pairs, ((*o*-piv)$_4$TPP)Fe(*N*-MeIm)$^+Cl^-$. Smaller downfield pyrrole H and upfield piv $CH_3$ shifts (Table II) are consistent with a decrease in the dipolar contribution to the isotropic shift, and thus we expect that *N*-MeIm produces a smaller zero-field splitting constant than does $Cl^-$.[28]

There are no additional peaks in the spectrum of sample II (Figure 4) or of sample I in the region between the coordinated *N*-MeIm resonances (20 ppm) and the high-spin Fe(III) pyrrole H resonances at 79 ppm. Thus, there is no evidence of a 6-coordinate (chloride-bound) high-spin form of the mono(*N*-MeIm) complex of the atropisomers of ((*o*-piv)$_4$TPP)FeCl. If it existed, it should have its pyrrole H resonance near 65 ppm, by analogy to the high-spin bis($Me_2SO$) complex of (TPP)$Fe^{III}$.[36] Such a high-spin, chloride bound, mono(*N*-MeIm) complex has been proposed as the major intermediate in the formation of (TPP)-Fe(*N*-MeIm)$_2^+Cl^-$.[37] The formation constant of this species has been estimated to be 3 $M^{-1}$ in $CH_2Cl_2$ by indirect spectroscopic methods during stopped-flow kinetic studies.[37] In contrast, estimates of the formation constant for the mono(*N*-MeIm) complex of (TPP)FeCl by direct spectrophotometric methods ($K_{eq}$ = 88 $M^{-1}$ "within a factor of two")[33] and by electrochemical techniques ($K_{eq}$ = 27 ± 10 $M^{-1}$)[38] in the same solvent are considerably larger. These results have led to the suggestion that the "chloride-off" form of the mono(*N*-MeIm) complex of (TPP)FeCl is the major thermodynamically stable one, and the "chloride-on" form is the minor one.[37] Additional NMR studies of the reaction of (TPP)FeCl with very low concentrations of *N*-MeIm at various temperatures and high magnetic field strength (to suppress chemical exchange effects due to phenyl rotation[24,29] or metal "inversion"[31]) could potentially provide a resolution of the question of coordination number of the mono(*N*-MeIm) complex of that compound, as it appears to have done for ((*o*-piv)$_4$TPP)FeCl.

Returning to the three atropisomers of the bis(*N*-MeIm) complex of ((*o*-piv)$_4$TPP)$Fe^{III}$ and their NMR spectra (Figure 5), let us dispense first with discussion of the $\alpha\alpha\alpha\beta$ isomer. We would expect it to be quite hindered in its ability to bind the second ($\alpha\alpha\alpha$ side) *N*-MeIm ligand, and hence require a higher concentration of that ligand than either the $\alpha\beta\alpha\beta$ or $\alpha\alpha\beta\beta$ atropisomers. The probable orientation of the second ligand's plane, once coordinated, is difficult to predict. It is also likely subject to more rapid on–off kinetics than those of the $\alpha\beta\alpha\beta$ and $\alpha\alpha\beta\beta$ isomers. Furthermore, the $\beta$-side ligand can probably rotate at least 90° before ecountering the single $\beta$-*o*-pivalmido group (Figure 1c). Because of the steric hindrance to binding of *N*-methylimidazole to the $\alpha\alpha\alpha$ side, the bond strength of that ligand is probably different from those of the other isomers, thus leading to a different average ligand field effect of *N*-MeIm for the $\alpha\alpha\alpha\beta$ isomer, which could displace its pyrrole resonances from the center of gravity observed for the $\alpha\beta\alpha\beta$ and $\alpha\alpha\beta\beta$ isomers.[34]

Of the three remaining pyrrole H resonances, we can assign that at −18.6 ppm to the $\alpha\beta\alpha\beta$ isomer, and the pair, at −17.1 and −20.0 ppm, to the $\alpha\alpha\beta\beta$ isomer, based upon comparison of the relative intensities of these peaks to the ratio of $\alpha\beta\alpha\beta$ to $\alpha\alpha\beta\beta$ present before metal insertion. For example, the ratios obtained from the areas of the three peaks of interest for sample I, Figure 5c, is ca. 1:1, while that for sample II, Figure 5e, is ca. 1:2.6, as compared to 1:1 and 1:2.3, respectively, originally present for the metal-free samples I and II.

The fact that, based upon the ratio of intensities of the central and outer peaks, we may assign those pyrrole H resonances to the $\alpha\beta\alpha\beta$ and $\alpha\alpha\beta\beta$ atropisomers, respectively, is proof of the hypothesis that axial ligand planes can lift the degeneracy of the metal $d_\pi$ and porphyrin $3e(\pi)$ orbitals into which the electron is delocalized. The same substituent is present on each phenyl ring, thus eliminating the "unsymmetrical substituent effect"[18,19] from consideration as the reason for the splitting of the pyrrole H resonance of the $\alpha\alpha\beta\beta$ isomer. And although the symmetry respresentation of the two isomers is different, even in the absence of axial ligands ($D_{2d}$ for $\alpha\beta\alpha\beta$ vs. $C_{2h}$ for $\alpha\alpha\beta\beta$), this difference does not cause inequality of the pyrrole protons in either the high-spin Fe(III) or metal-free forms of the two isomers.[39] Thus the splitting of the pyrrole H resonance of the $\alpha\alpha\beta\beta$ isomer of ((*o*-piv)$_4$TPP)Fe(*N*-MeIm)$_2^+$ must be due to lifting the degeneracy of the $3e(\pi)$ orbitals by restricting the rotation of the axial ligands so as to place them in the same plane.

If we assume that the axial *N*-methylimidazole ligands of the two atropisomers are forced to sit, on the average, as shown in

(35) Statterlee, J. D.; LaMar, G. N. *J. Am. Chem. Soc.* **1976**, *98*, 2804–2808.
(36) Zobrst, M., LaMar, G. N. *J. Am. Chem. Soc.* **1978**, *100*, 1044–1046.
(37) Burdige, D.; Sweigert, D. A. *Inorg. Chim. Acta*, **1979**, *28*, L131. Fiske, W. W.; Sweigart, D. A. *Ibid.* **1979**, *36*, L429.
(38) Walker, F. A.; Barry, J. A.; Balke, V. L.; McDermott, G. A.; Wu, M. Z.; Linde, P. f., *Adv. Chem. Ser.*, **1982**, *No. 201*, 377–416.

(39) An obvious experiment, which might have further clarified the role of the $3e(\pi)$ orbitals, but instead only complicated the issue, was to compare the NMR spectra of the bis(*N*-MeIm) complexes to those of the bis-cyanide complexes of the atropisomeric mixtures of ((*o*-piv)$_4$TPP)$Fe^{III}$. The absence of axial ligand planes should cause the four peaks observed for samples I and II (Figure 5) to collapse to a single resonance for the bis-cyanide complexes. However, the spectra observed for samples I and II in both $CD_3OD$ and $Me_2SO$-$d_6$ in the presence of excess KCN consisted of at least five closely spaced, overlapping peaks (−16.7 to −17.2 ppm at 22 °C in $CD_3OD$ at 200 MHz), whose intensity ratios varied significantly with temperature in a manner which was not consistent with any interpretation of the atropisomeric ratios present in each sample. Additionally, a small peak (3% of the total) was present at −18.4 ppm, at 22 °C, which did not change in intensity as the temperature was varied and whose isotropic shift showed Curie behavior. Earlier NMR studies of $PFe(CN)_2$–complexes[40] as a function of solvent pointed out the importance of H-bonding between solvent and the coordinated cyanides on the observed isotropic shifts of porphyrin protons. We believe that the variable-temperature behavior of the intensities and isotropic shifts of the "at least five" closely spaced overlapping pyrrole H resonances of samples I and II when coordinated to $CN^-$ are indicative of temperature-dependent equilibria involving H-bond donation by the N–H protons of the pivalamido groups, and, in the case of $CD_3OD$, competition of these N–H protons with solvent for H-bond donation to $CN^-$. Such H-bond donation from the pivalamido N–H protons could affect the pattern of pyrrole H resonances in two ways: (a) by changing the base strength of the coordinated CN ligands and thereby changing the isotropic shift and (b) by bending the $CN^-$ toward a given N–H, thereby imposing a plane of symmetry that would lift the degeneracy of the $3e(\pi)$ orbitals. The small peak at −18.4 pm might thus be due to the presence of a small amount of the $\alpha\alpha\alpha\alpha$ atropisomer, where four equal N–H interactions are possible on one side, but only solvent interactions are possible with the $\beta$-side $CN^-$. (Such interactions between the N–H protons of the pivalamido groups and the N–$CH_3$ nitrogen of *N*-MeIm are expected to be extremely weak or nonexistent due to the involvement of the N–$CH_3$ lone pair in the $\pi$ system of the imidazole, and thus N–H → *N*-MeIm H-bond donation cannot explain the existence of the four peaks of Figure 5.)
(40) LaMar, G. N.; Del Gaudio, J.; Frye, J. S. *Biochim. Biophys. Acta* **1977**, *498*, 422–435.

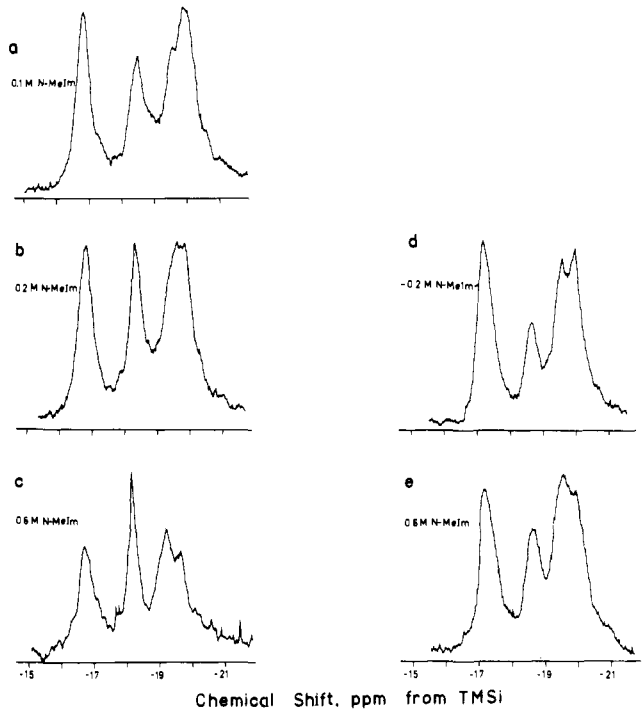


**Figure 5.** *N*-Methylimidazole concentration dependence of the pyrrole H resonances of two low-spin $((o\text{-Piv})_4\text{TPP})\text{Fe}(N\text{-MeIm})_2^+$ samples.[32,34] The sample shown in parts a–c was sample I, which had 1:1 ratio of $\alpha\beta\alpha\beta$:$\alpha\alpha\beta\beta$ isomers before insertion of iron, while that in parts d and e was sample II, which had a 1:2.3 ratio of isomers. Spectr recorded at 200 MHz in $CDCl_3$: parts a–c at 22 °C, parts d and e at 21 °C.

Figure 1a,b, then the effect upon the 3e($\pi$) orbitals of the porphyrin is expected to be as shown in Figure 1d,e. For the $\alpha\alpha\beta\beta$ isomer (Figure 1a), the axial ligand planes are parallel and lie over two opposite nitrogens. Thus one 3e($\pi$) porphyrin orbital can interact with the filled $\pi$ orbitals of both axial imidazoles while the other, which lies at a 90° angle to the one shown in Figure 1d, cannot interact with either axial ligand. This raises the energy of the orbital shown in Figure 1d, since it too is filled, and leads to its being favored for unpaired electron delocalization by porphyrin → Fe $\pi$-back-bonding.[2-4] This creates two very different spin densities at symmetrically related pyrrole positions, as indicated by the different sizes of the circles of the right- and left-hand, as compared to the top and bottom pyrrole rings. The pyrrole proton resonance is thus split into two peaks. By analogy to the unsymmetrically substituted $(\text{TPP})\text{Fe}(N\text{-MeIm})_2^+$ complexes whose pyrrole resonances we have assigned[19] (and whose assignments we have confirmed through study of their temperature dependences[41]), we assign the resonance near −20 ppm to the right- and left-hand pyrrole ring protons and the resonance near −17 ppm to the top and bottom pyrrole ring protons of Figure 1a,d.[42]

For the $\alpha\beta\alpha\beta$ isomer of Figure 1b, the axial ligand planes are, on the average, perpendicular to each other and lie along the meso positions, as shown. Both 3e($\pi$) orbitals are thus equally populated because of the perpendicular alignment of the axial ligands, and the overlapping orbital electron density distribution is as shown in Figure 1e. Thus the pyrrole protons all have identical spin densities and only one pyrrole proton resonance is observed. Since the average of the two spin densities of the orbital utilized by the $\alpha\alpha\beta\beta$ isomer is the same as that of the $\alpha\beta\alpha\beta$ isomer, the two pyrrole H peaks of the former are equally displaced upfield and downfield that of the latter.

The NMR spectra shown in Figure 5 confirm the hypothesis that, in the absence of effects due to unsymmetrically placed substituents, the axial ligand plane(s) is (are) responsible for splitting the degeneracy of the 3e($\pi$) molecular orbitals of the porphyrin, and thus splitting the pyrrole proton resonance of symmetrically substituted porphyrins. The present studies of this one sterically hindering ortho substituent, the pivalamido group, do not allow us to determine how rigidly perpendicular the ligands are held in the $\alpha\beta\alpha\beta$ isomer or how rigidly parallel in the $\alpha\alpha\beta\beta$ isomer, but only that, on the average, the ligand planes are perpendicular and parallel, respectively. Thus the ca. 2.9 ppm splitting of the pyrrole protons of the $\alpha\alpha\beta\beta$ isomer may not represent the maximum possible.[31] Molecular models indeed suggest that the tert-butyl group of the pivalamido substituent is too far above the plane of the porphyrin, on the average, to have the maximum possible effect on holding the axial ligands rigidly in place. We are currently preparing additional pairs of isomers with more bulky and differently shaped ortho substituents in order to determine the maximum possible splitting of the pyrrole proton resonances. It is hoped that the $\alpha\beta\alpha\beta$ and $\alpha\alpha\beta\beta$ isomers of these compounds will be more readily separable, which will allow measurement and comparison of the redox potentials and other physical properties of the parallel and perpendicular forms.

## Summary

The assignment of the pyrrole H resonances of the bis(N-methylimidazole) complexes of mixtures of the $\alpha\beta\alpha\beta$ and $\alpha\alpha\beta\beta$ atropisomers of $((o\text{-piv})_4\text{TPP})\text{Fe}^{\text{III}}$ is made on the basis of their intensity ratio to the ratio of $\alpha\beta\alpha\beta$ to $\alpha\alpha\beta\beta$ found for the metal-free precursors.

The low-spin $\alpha\alpha\beta\beta$ atropisomer should, by virture of the placement of bulky *o*-pivalamido groups on two adjacent phenyls on each side of the porphyrin plane, have its *N*-methylimidazole ligands lying in the same plane (parallel to each other), over two opposite porphyrin nitrogens, thus imposing a single plane of symmetry on the porphyrin ring. In contrast, the $\alpha\beta\alpha\beta$ atropisomer should have its *N*-methylimidazole ligands lying in perpendicular planes, thus imposing two 90° planes of symmetry on the porphyrin ring. Since the unpaired electron of low-spin Fe(III) is delocalized into e-symmetry porphyrin $\pi$ orbitals,[2-4] the parallel orientation of axial ligand planes in the $\alpha\alpha\beta\beta$ atropisomer lifts the degeneracy of the 3e($\pi$) orbitals, leading to two very different unpaired electron densities at pyrrole carbons, and two pyrrole H NMR peaks. In contrast, the perpendicular arrangement of axial ligand planes in the $\alpha\beta\alpha\beta$ atropisomer maintains the degeneracy of the 3e($\pi$) orbitals and leads to equal electron density at all pyrrole carbons and only one pyrrole H NMR peak.

**Acknowledgment.** The financial support of NSF (CHE 79-18217), NIH (AM 31038), NIH RCDA (GM 00227) (F.A.W.), and NIH Minority High School Research Apprentice Program (1 503 RR0316-1) (J.T.W.) is gratefully acknowledged. We thank Drs. L. Latos-Grazynski, G. N. LaMar, and A. L. Balch for providing the *m*-H shift information for $(\alpha\alpha\alpha\alpha\text{-}(o\text{-piv})_4\text{TPP})\text{FeBr}$ prior to publication. This work is part of the M.S. degree project of J.B.

**Registry No.** $\alpha\beta\alpha\beta\text{-}(o\text{-piv})_4\text{TPPH}_2$, 77027-26-0; $\alpha\alpha\beta\beta\text{-}(o\text{-piv})_4\text{TPPH}_2$, 77027-27-1; $\alpha\alpha\alpha\beta\text{-}(o\text{-piv})_4\text{TPPH}_2$, 77027-25-9; $\alpha\alpha\alpha\alpha\text{-}(o\text{-piv})_4\text{TPPH}_2$, 55253-62-8; $\alpha\beta\alpha\beta\text{-}((o\text{-piv})_4\text{TPP})\text{FeCl}$, 87334-91-6; $\alpha\alpha\beta\beta\text{-}((o\text{-piv})_4\text{TPP})\text{FeCl}$, 87334-92-7; $\alpha\alpha\alpha\beta\text{-}((o\text{-piv})_4\text{TPP})\text{FeCl}$, 87334-93-8; $\alpha\alpha\alpha\alpha\text{-}((o\text{-piv})_4\text{TPP})\text{FeCl}$, 86107-94-0; $\alpha\beta\alpha\beta\text{-}((o\text{-piv})_4\text{TPP})\text{Fe}(N\text{-MeIm})_2^+\text{Cl}^-$, 87306-15-8; $\alpha\alpha\beta\beta\text{-}((o\text{-piv})_4\text{TPP})\text{Fe}(N\text{-MeIm})_2^+\text{Cl}^-$, 87334-94-9; $\alpha\alpha\alpha\beta\text{-}((o\text{-piv})_4\text{TPP})\text{Fe}(N\text{-MeIm})_2^+\text{Cl}^-$, 87334-95-0; $\alpha\beta\alpha\beta\text{-}(o\text{-NH}_2)_4\text{TPPH}_2$, 68070-28-0; $\alpha\alpha\beta\beta\text{-}(o\text{-NH}_2)_4\text{TPPH}_2$, 68070-29-1; $((o\text{-piv})_4\text{TPP})\text{Fe}(N\text{-MeIm})^+\text{Cl}^-$, 87306-16-9.

(41) Walker, F. A.; Benson, M. *J. Phys. Chem.* **1982**, *86*, 3495–3499.

(42) An alternative assignment is possible if the empty $\pi^*$ orbitals of *N*-MeIm (rather than the filled $\pi$ orbitals) are similar in energy to the 3e($\pi$) porphyrin orbitals. In this case, interaction of the $\pi^*$ orbitals of the two *N*-MeIm with the 3e($\pi$) porphyrin orbital shown in Figure 1d would lower the energy of this orbital, leaving the other 3e($\pi$) orbital to be favored for unpaired electron delocalization through porphyrin → Fe $\pi$-back-bonding. This would lead to the assignment of the resonance near −20 ppm to the top and bottom pyrrole ring protons and the resonance near −17 ppm to the right- and left-hand pyrrole ring protons of Figure 1a, since the 3e($\pi$) orbital at right angles to that shown in Figure 1d would be the one utilized for unpaired electron delocalization. This assignment seems less likely than that presented in the text, since the $\pi$ orbital ionization energies of imidazoles are smaller than the lone pair ionization energies,[43] indicating that imidazoles are better $\pi$ donors than acceptors.

(43) Ramsey, B. G. *J. Org. Chem.* **1979**, *44*, 2093–2097.